


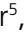




Integrated Seismic Program (ISP): A New Python GUI-Based Software for Earthquake Seismology and Seismic Signal Processing

Roberto Cabieces¹, Andrés Olivar-Castaño², Thiago C. Junqueira³,
Jesús Relinque¹, Luis Fernandez-Prieto⁴, Jiří Vackár⁵, Boris Rösler⁶,
Jaime Barco⁷, Antonio Pazos¹, and Luz García-Martínez⁸

Abstract

Integrated Seismic Program (ISP) is a graphical user interface designed to facilitate and provide a user-friendly framework for performing diverse common and advanced tasks in seismological research. ISP is composed of five main modules for earthquake location, time–frequency analysis and advanced signal processing, implementation of array techniques to estimate the slowness vector, seismic moment tensor inversion, and receiver function computation and analysis. In addition, several support tools are available, allowing the user to create an event database, download data from International Federation of Digital Seismograph Networks services, inspect the background noise, and compute synthetic seismograms. ISP is written in Python3, supported by several open-source and/or publicly available tools. Its modular design allows for new features to be added in a collaborative development environment.

Cite this article as Cabieces, R., A. Olivar-Castaño, T. C. Junqueira, J. Relinque, L. Fernandez-Prieto, J. Vackár, B. Rösler, J. Barco, A. Pazos, and L. García-Martínez (2022). Integrated Seismic Program (ISP): A New Python GUI-Based Software for Earthquake Seismology and Seismic Signal Processing, *Seismol. Res. Lett.* **93**, 1895–1908, doi: [10.1785/SR202210205](https://doi.org/10.1785/SR202210205).

[Supplemental Material](#)

Introduction

Seismic programs have been commonly designed by seismologists to help analyze large amounts of data and implement complex workflows. In addition, they are used to create models such as synthetic seismograms, and to run routines that require visualization for inspection (e.g., earthquake location and focal mechanisms).

The usability of a software depends strongly on its installability, performance, and robustness. Most of the freely available and widely used seismic programs such as Seismic Handler, Seismic Analysis Code, or Computer Programs in Seismology (Stammler, 1993; Goldstein *et al.*, 2003; Herrmann, 2013) are command line tools. Although appropriate for automating repetitive tasks, command line tools generally have a steep learning curve and require certain expertise to be used efficiently. Software packages with a graphical user interface (GUI) are usually more intuitive, and thus usable even for beginner-level users, and facilitate tasks that require user interaction.

Recently, open-source software such as SeisGram2K (see [Data and Resources](#)), SEISAN or Geopsy (Havskov *et al.*, 2020; Wathelet *et al.*, 2020) that partially provide GUIs have been published, which make it possible for users to analyze seismic data without previous knowledge in programming or the necessity to use the terminal to run software commands. However, these programs execute multiple tasks in a single

toolbox. This nonmodular design makes it difficult to maintain the software and continue its development past its intended use. On the other hand, programming language libraries such as ObsPy (Krischer *et al.*, 2015), dedicated to managing seismic data, lack interactivity between the user and the graphical part of the software, for example, to retrieve data directly through a graphical interface, and inhibit introspection of the code to change default algorithm parameters.

Integrated Seismic Program (ISP) is a set of GUI-equipped toolboxes (Fig. 1) for which the main objective is to offer an interactive and amendable environment for earthquake seismology and signal processing. ISP offers five independent modules in the current version, each performing a common seismological

1. Department of Geophysics, Spanish Navy Observatory, San Fernando, Spain, <https://orcid.org/0000-0003-2602-5014> (RC); <https://orcid.org/0000-0002-1912-9336> (JR); 2. Department of Geology, Universidad de Oviedo, Oviedo, Spain, <https://orcid.org/0000-0002-5957-942X> (AO-C); 3. Institute of Geoscience, University of Potsdam, Potsdam-Golm, Germany; 4. Institute of Marine Sciences, Barcelona, Spain, <https://orcid.org/0000-0001-9355-0113> (LF-P); 5. Institute of Rock Structure and Mechanics, Czech Academy of Sciences, Prague, Czechia; 6. Department of Earth and Planetary Sciences, Northwestern University, Evanston, Illinois, U.S.A., <https://orcid.org/0000-0001-8596-5650> (BR); 7. Seismology Department, Instituto Geográfico Nacional, Madrid, Spain; 8. Department of Signal Theory, Telematics and Communications, University of Granada, Granada, Spain, <https://orcid.org/0000-0001-5904-5412> (LG-M)

*Corresponding author: rcabdia@roa.es

© Seismological Society of America

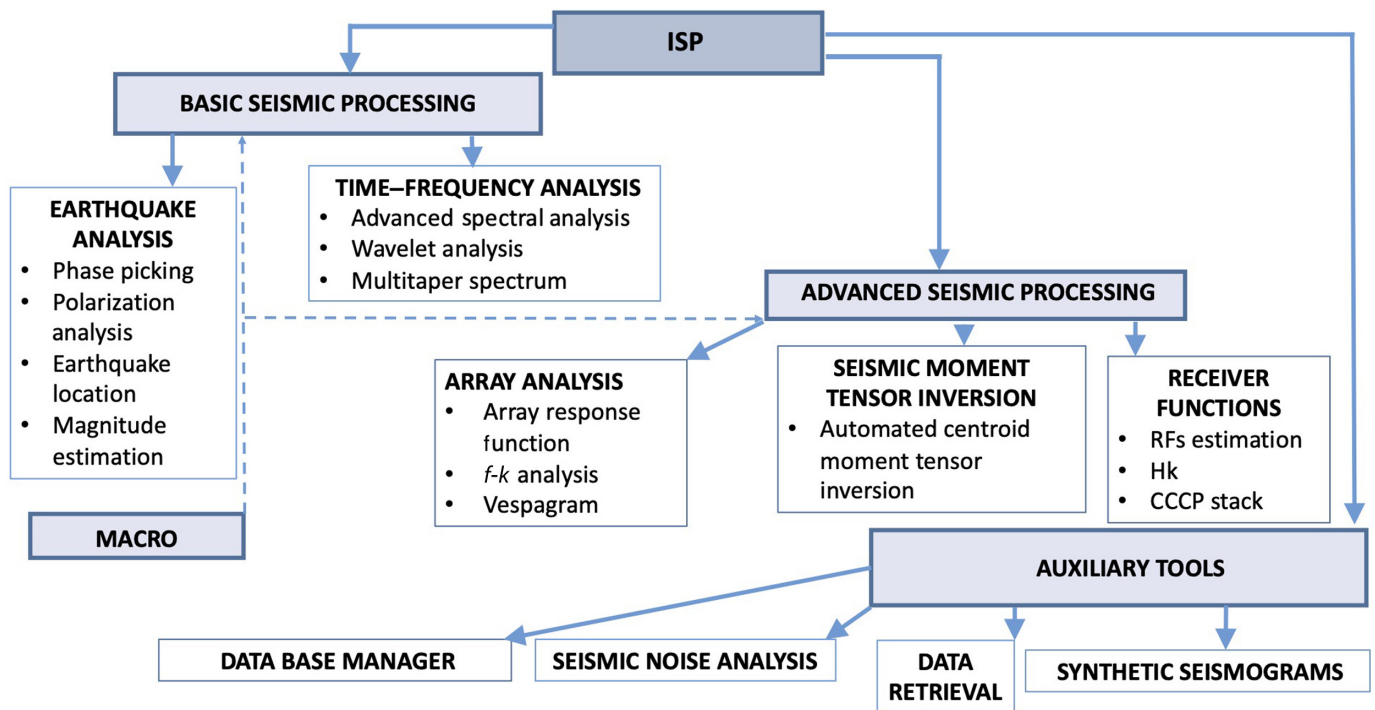


Figure 1. Integrated Seismic Program (ISP) framework. General scope of software modules and auxiliary tools. RF, Receiver Function. The color version of this figure is available only in the electronic edition.

research task, and several accompanying tools that allow the user to create an event database, retrieve data from International Federation of Digital Seismograph Networks (FDSN) services, and compute probability power spectral density functions (PPSDs) and synthetic seismograms.

ISP is written in Python and uses the PyQt5 library (see [Data and Resources](#)), which is commonly used for GUI development. The ObsPy library is used for data download routines, several signal processing methods, and read and write support for different seismological data formats. ISP incorporates three third-party software packages, with permission from their respective authors: NonLinLoc ([Lomax and Curtis, 2001](#)) for earthquake location using 3D velocity models ([Silva et al., 2017](#); [Cabiesces et al., 2020](#)), Bayesian ISOLated Asperities (ISOLA; [Vackář et al., 2017](#)) for centroid moment tensor (CMT) inversion, and the classic FOCal MECHANism determinations (FOCMEC) software (see [Data and Resources](#)) for determining and displaying double-couple earthquake focal mechanisms using the polarity and amplitude ratios of *P* and *S* waves.

The ISP project is focused on the transparency of the code and its development ([Smith et al., 2018](#)) and provides an intuitive documentation of the software. Its availability through GitHub (see [Data and Resources](#)), a website designed for software version control, provides access to the current version of the code and updated software documentation. Tracking and version control are achieved through Git ([Loeliger and McCullough, 2012](#)). The ISP documentation was created using MkDocs (see [Data and Resources](#)) and is linked to the ISP GitHub project, thus enabling direct access for the end user through a web browser or their own software. ISP is a free

open-software licensed under the GNU Lesser General Public License version 3.0 (v.3.0).

In the following sections, we describe the modular structure of ISP and the functionality of each toolbox.

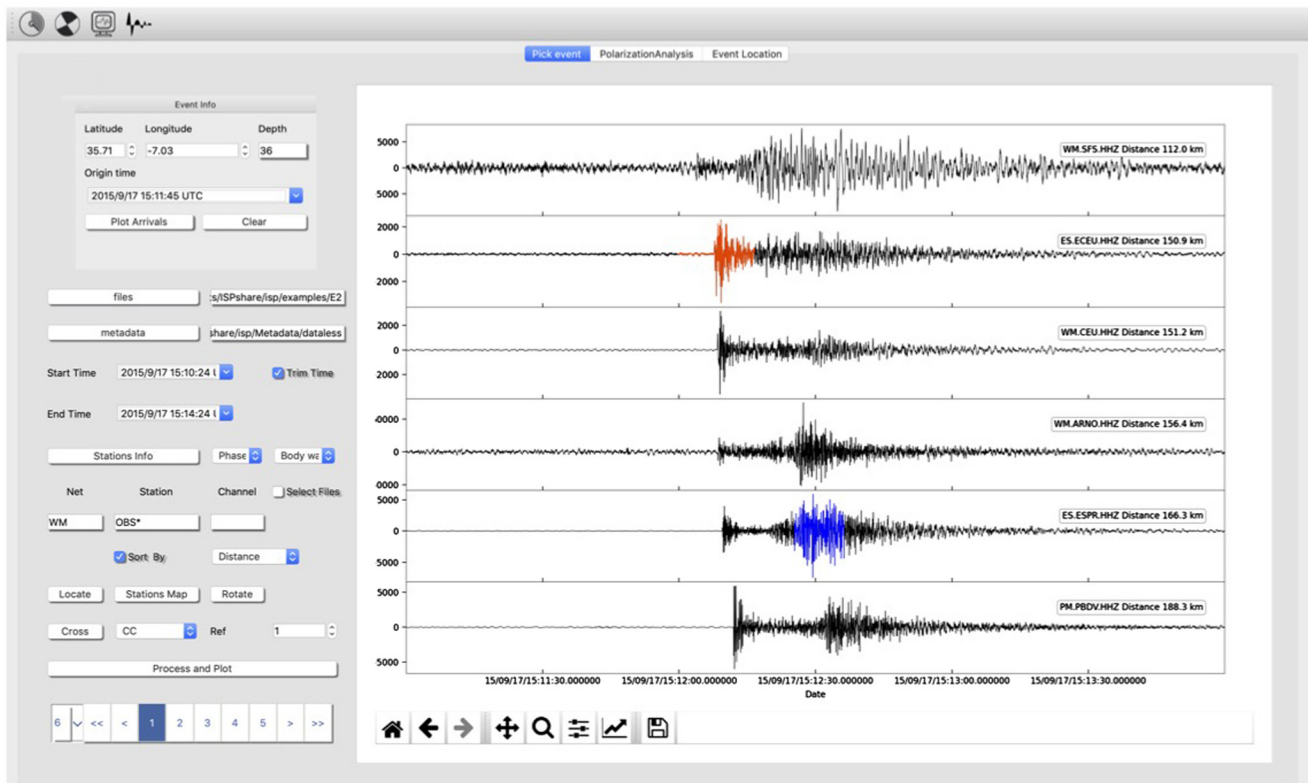
Main ISP Modules

Earthquake analysis

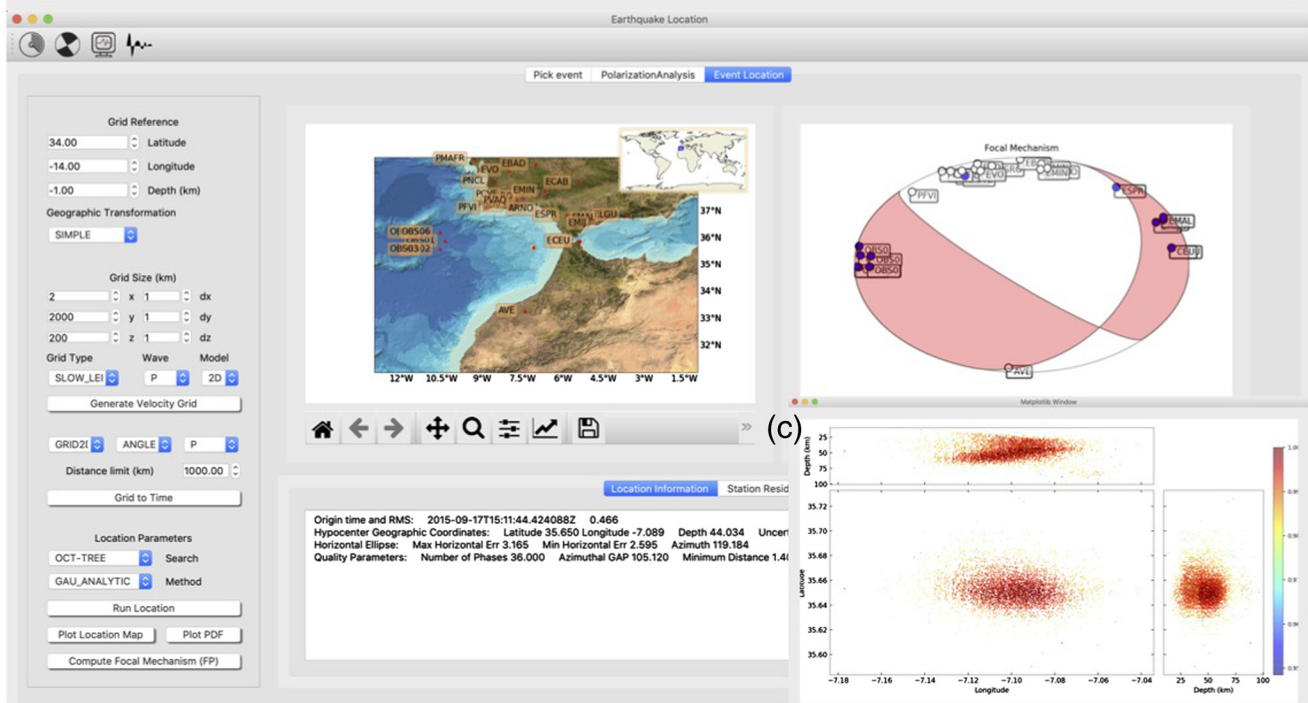
The earthquake analysis module allows earthquake location, magnitude estimation, polarization analysis, and focal mechanism determination using the polarity of *P* and *S* waves. The focal parameters obtained with this module form the basis for further analysis of the event with ISP. The GUI of the earthquake analysis module is divided into three different frames to pick an event, perform polarization analysis, and locate the event.

Figure 2 shows the frames to pick an event (Fig. 2a) and locating it (Fig. 2b). In the former, the user has loaded and processed six waveforms and selected time windows corresponding to body waves (red) and surface waves (blue). In this frame, the seismic phases can be identified either manually or automatically using different picking algorithms, based on the energy of the seismic signal using the continuous wavelet transform (CWT; [Cabiesces et al., 2020](#)), the trace envelope and the spectral entropy, or using a neural network trained on more than 20,000 local, regional, and teleseismic events ([Ross et al., 2018](#)). The software is designed to easily incorporate additional neural networks.

(a)



(b)



The arrival times and first-motion polarity of the different phases can be marked in the metadata header of each trace and saved to a file for later use during locating the event and determining its focal mechanism. In addition, the event picking frame provides a dedicated tool for magnitude estimation that implements the methodology introduced by Bormann and Dewey (2012). Preprocessing (i.e., filtering, tapering, detrending, etc.) of the seismic waveforms is handled by the fully

Figure 2. Earthquake analysis module, (a) event picking frame, (b) event location frame showing the results of a regional earthquake and its focal mechanism obtained from first motions, and (c) probability density function of the earthquake location search. The color version of this figure is available only in the electronic edition.

customizable macro processing tool (for further details, see the [Macros for seismic signal processing](#) section).

The polarization analysis tool (Fig. S1, available in the supplemental material to this article) can be used to rotate the data to the ZRT or LQT reference systems. The particle motion for the determination of the polarization angles of the waveforms is analyzed following [Flinn \(1965\)](#). This approach allows characterizing the temporal evolution of the azimuth and incidence angle with the planarity and/or rectilinearity.

The event location frame (Fig. 2b,c) provides a GUI for the well-known nonlinear location (NLL) algorithm ([Lomax and Curtis, 2001](#)). This algorithm allows locating events using either a 1D or 3D Earth velocity model based on direct search methods such as the stochastic Metropolis-Gibbs ([Sambridge and Mosegaard, 2002](#)) or the Oct-tree sampling algorithm ([Lomax and Curtis, 2001](#)). NLL uses the Eikonal finite-difference algorithm implemented by [Podvin and Lecomte \(1991\)](#) to estimate the travel times and complete probabilistic solution through the equivalent differential time ([Zhou, 1994](#); [Font et al., 2004](#)).

The event location frame also contains the FOCMEC software (see [Data and Resources](#)) for the computation of focal mechanisms, which allows obtaining a fast and reliable estimation of the fault planes and their uncertainties for events with good station coverage. The input parameters are retrieved from the output file generated by the earthquake location routines containing the first arrival polarities picked by the user. To help the user select the parameters used for the computation of synthetic travel times, the earthquake analysis module includes a tool for visualizing 3D velocity models. The hypocenter location, fault-plane solution, and magnitude estimate along with their corresponding uncertainties can be saved in an SQLite database (further details in the [Event database](#) section) for later use to compile statistics.

Time–frequency analysis

The main purpose of the time–frequency analysis module is to provide a quick and convenient way of representing signals in the time–frequency domain. This module provides dedicated signal processing tools such as the CWT ([Daubechies, 1992](#); [Torrence and Compo, 1998](#); [Mallat, 2009](#)) using the Morlet, Paul, and Mexican Hat wavelets, the possibility of computing a multitaper spectrogram ([Thomson, 1982](#); [Prieto et al., 2009](#)) and the Wigner–Ville distributions ([Boashash and Black, 1987](#)), among others.

The tools provided by this module facilitate comparisons between two signals using the power spectrum, magnitude square coherence, transfer function, cross- and autocorrelation, and cross-continuous wavelet, among other methods.

Figure 3 shows a screenshot of the GUI of this module, in which the time–frequency domain representation of a regional earthquake (Fig. 3a files selector and plotting parameters), has

been computed at two different stations, using the CWT (Fig. 3b) and the multitaper spectrogram (Fig. 3c). The parameters used for the computation of the time–frequency representation, as well as different plotting methods, can be easily changed in the bottom-left area of the GUI (Fig. 3d parametrization widgets).

Array analysis

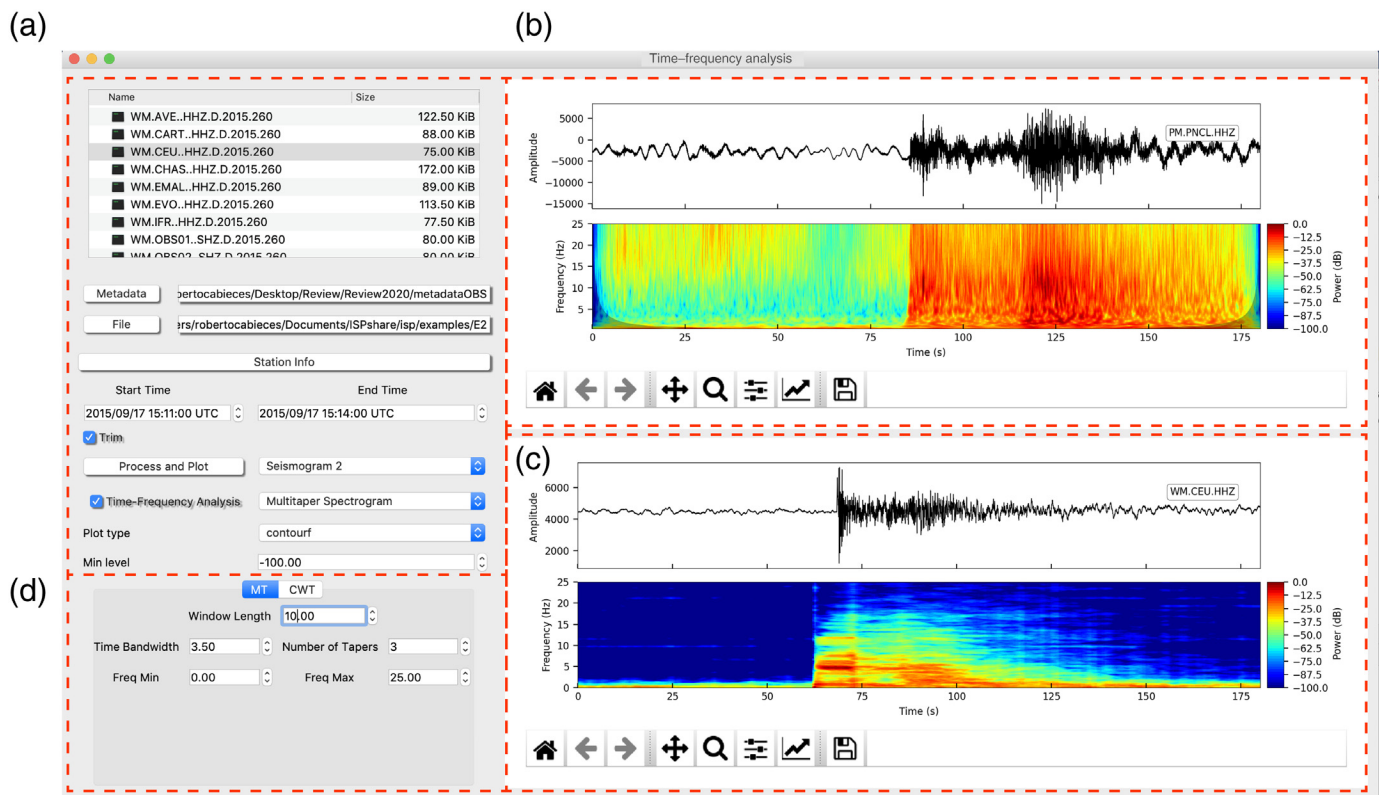
The design of this module is aimed at researchers and institutions managing seismic arrays using common array techniques to study regional and teleseismic events. The array analysis module includes tools to determine the array response function (ARF; [Nawab et al., 1985](#); [Ruigrok et al., 2017](#)), the frequency–wavenumber (f - k ; [Capon, 1969](#); [Gal et al., 2014](#)) analysis, and the Vespagram ([Rost and Thomas, 2002](#)). Figure 4 shows an example in which the f - k frame has been used to analyze the 2017 North Korea nuclear test from the Eielson Alaska Long Period Array Research. In the left panels (Fig. 4a), the user configures the f - k parameters and displays the slowness map of a time window (Fig. 4b). On the right panels, the temporal evolution of the f - k analysis (Fig. 4c) and the stack for a specific time window (Fig. 4d) are shown.

In the first frame of this module (Fig. S2), the user has the option to compute the ARF, which helps to design the geometry of an array, given the wave parameters slowness or wavenumber and the frequency range. The estimation of the ARF is intended to optimize the configuration parameters for f - k analysis. In the second frame, the f - k analysis is used to estimate the slowness vector using overlapping time windows. The broadband f - k spectrum can be computed using the conventional method or using the multitaper coherence algorithm ([Prieto et al., 2009](#)). This method differs from the conventional methods in the tapering of the time windows ([Thomson, 1982](#)). In the multitaper method, the signals are convolved with the discrete prolate spheroidal sequences, which generally decreases the variance of the spectral estimates. This improved accuracy reduces the size of the main lobe in the f - k slowness map, which in turn improves the slowness vector estimation. In addition, waveform stacking can be done using different algorithms (linear, n th root, or phase weight stack; [Schimmel and Paulssen, 1997](#); [Ventosa et al., 2017](#)), according to the slowness vector with the maximum relative power or coherence.

The last tool included in this module is designed to compute the velocity spectral analysis. The vespagram (Fig. S3) time function allows establishing a slowness or a backazimuth and thereby obtaining the time-dependent f - k based on these parameters.

Seismic moment tensor inversion

ISP includes a module to perform a seismic moment tensor inversion. The functionality of this module is based on the Bayes-ISOLA code ([Vackář et al., 2017](#)), a tool for automated CMT inversion in a Bayesian framework. This module includes



a function to calculate an optional data covariance matrix from pre-event noise that yields an automatic weighting function for the receiver components according to their noise levels. This also serves as an automated frequency filter that suppresses noisy frequency ranges. During the inversion, a grid search is performed over time and space, combined with an analytical (least squares) moment tensor inversion at each grid point, which accelerates the inversion process. The more time-consuming tasks like the Green's function computation and the grid search are parallelized for efficiency. The results provided by the module contain the best-fit solution, as well as the full posterior probability density function (PPDF), which allows the user to plot the marginal probability density functions (PDFs) for any of the CMT parameters. This method provides a best-fitting CMT solution and a full (non-Gaussian) PPDF (Sambridge and Mosegaard, 2002; Sambridge, 2013).

Figure 5 shows the main window of the moment tensor inversion module. The widgets in the left panel allow (Fig. 5a) the user to change the inversion parameters. The results of the inversion are shown in the right panel (Fig. 5b).

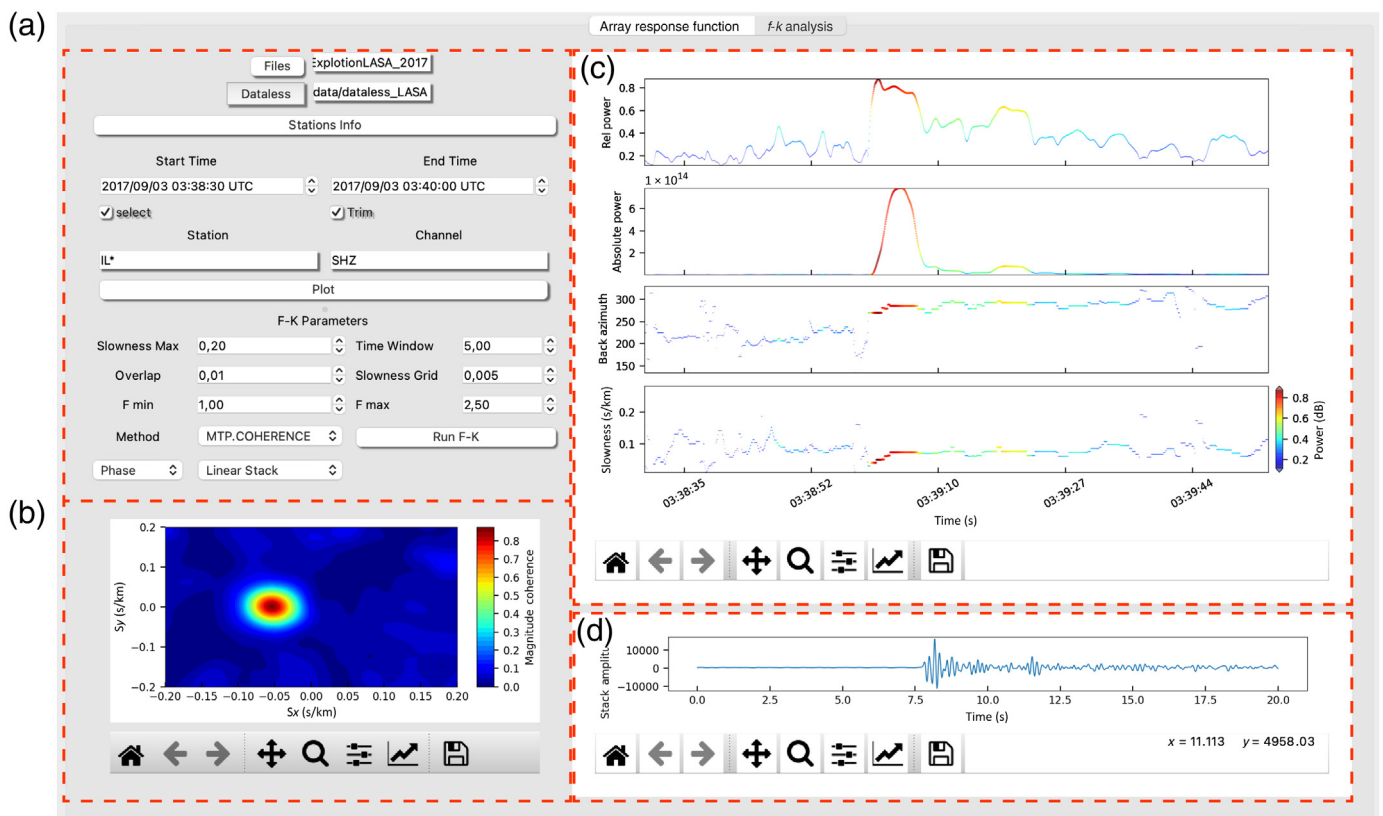
The moment tensor inversion module also handles data preprocessing using the macro tool (for details, see the [Macros for seismic signal processing](#) section subsequently), and includes a graphic tool to create 1D Earth velocity models to be used in the inversion. The GUI allows the user to select the frequency range and grid size, to calculate the data covariance matrix, and to filter receiver components, giving full control over the inversion process.

Figure 3. Time–frequency analysis module. (a) Files selector and plotting parameters, (b) time–frequency energy plane of a seismogram from the continuous wavelet transform using the Morlet wavelet, (c) time–frequency energy plane from the multitaper spectrogram for a different waveform, and (d) parameterization widgets. The color version of this figure is available only in the electronic edition.

Receiver functions

The receiver functions module computes and analyzes receiver functions. The GUI for this module is divided into two frames, which implement different analysis methods: H-k stacking and common conversion point (CCP) stacking (Fig. 6). Receiver functions are computed using the water-level deconvolution method (Langston, 1979) and are shown in the H-k stacking frame (Fig. 6a). This frame allows the user to choose the water-level parameter and the Gaussian filter width that can be used to apply a prior band-pass filter to the raw waveforms if necessary. The GUI provides a convenient way of performing visual quality control over the computed receiver functions and allows discarding selected receiver functions from further analysis. The remaining receiver functions can be used to determine the crustal thickness and the V_p/V_s ratio below the receiver using a semblance-weighted H-k stacking method (Zhu and Kanamori, 2000).

The CCP stacking of receiver functions is a method used to image the topography of subhorizontal interfaces below



the receivers. Receiver functions are treated as rays and, assuming a 1D velocity model, backprojected away from the receiver in the direction of the seismic source. At each step of this backprojection, the amplitudes of the receiver functions are assigned to their appropriate positions using a time-to-depth conversion. The 3D volume below the receivers is divided into a grid of regular cells, and the amplitude of the backprojected rays at any given depth is stacked into the cells inside the Fresnel zone of the ray at that depth. This procedure can be performed in the CCP stacking frame (Fig. 6b) using the receiver functions computed and saved in the H- k stacking frame. After loading the receiver functions, the positions of the receivers are shown on a map (Fig. 6b). The CCP stacking frame contains several parameters the user may edit such as the grid design (coordinates, maximum depth, and cell size) and the 1D model used for the backprojection of the rays. The user can interact with the map to design the grid for the backtracing (i.e., setting the grid boundaries) or to generate cross sections of the computed CCP stack (Fig. 6c).

Support tools

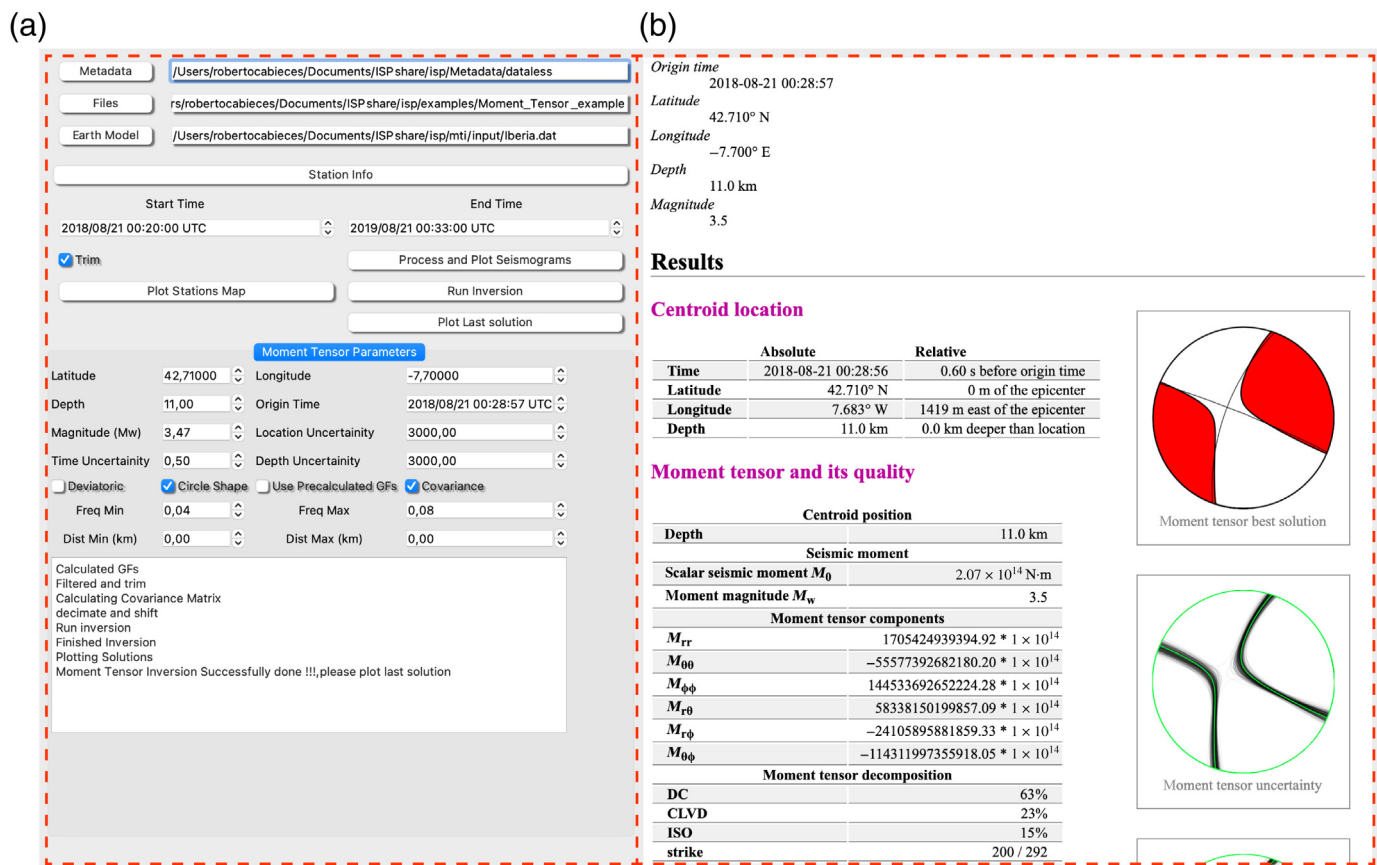
Macros for seismic signal processing. The macros are one of the most important parts of the ISP core and can be called from all the main modules to preprocess the raw seismograms. In ISP, the seismic signal processing (i.e., filtering, tapering, detrending, denoising, etc.) is carried out within the macro frame (Fig. 7) that allows the user to select the

Figure 4. Frequency–wavenumber (f - k) analysis in the array analysis module. Example of a slowness vector estimation from a nuclear explosion detection at the Eielson Alaska Long Period Array Research (ILAR) array in 2017. (a) Parameterization widgets, (b) slowness map, (c) time evolution f - k analysis, and (d) stack for a slowness vector test with the maximum power or coherence. The color version of this figure is available only in the electronic edition.

parameters for each processing step, as well as the order in which they are performed. The design of this frame facilitates tracking the signal processing and adjust its steps and their order.

The structure of the macro framework is as follows: the order of the process is set in the first column (Fig. 7a); additionally the user can remove or change the order of the process. The second column reports about the selected method (Fig. 7b), and the third column is designed to parameterize that method (Fig. 7c). The user can select and add more methods to the macro (Fig. 7d), and the complete signal processing macro can be saved for later use and loaded in all ISP modules (Fig. 7e).

Event database. The focal parameters of events located using the earthquake location module, as well as additional information including the slowness vector and CMT inversion results, can be saved in an SQLite database. This database can be accessed through a dedicated GUI (Fig. 8) to search and



manage the stored data. The user can filter the database, searching for events by period or study region (Fig. 8a). The result of the database query can be shown on a map (Fig. 8b), in which the user interaction is made possible through the table (Fig. 8c) that displays the selected data.

ISP uses SQLAlchemy (see Data and Resources) with an object relational mapping design. The main advantage of this design is that it allows easy conversion of the targeted database (i.e., PostgreSQL, Oracle, and SQLite). The main structure of the ISP database is shown in the Appendix.

PPSD analysis. This tool is aimed at evaluating the data acquisition performance of seismic stations through the estimation of PDFs (McNamara and Buland, 2004). PDFs are computed from locally stored data using the ObsPy library, and the results can be saved to a database for later use or loaded into the GUI, which offers multiple visualization options including displaying diurnal or seasonal plots. Diurnal seismic noise levels can be compared with the standard low- and high-noise models (Peterson, 1993, respectively) or with models for earthquakes of different magnitudes (Clinton and Heaton, 2002).

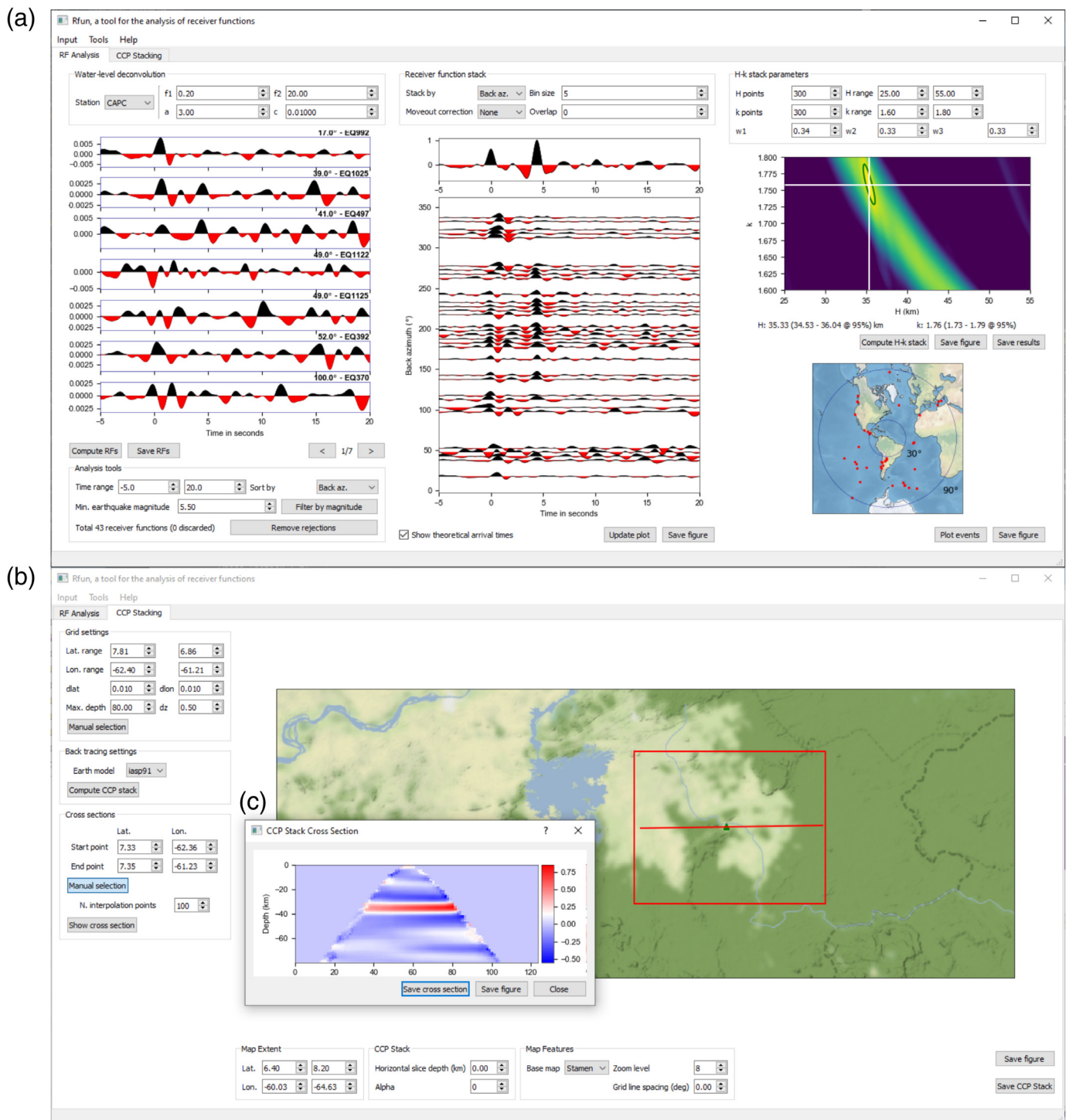
Figure 9 shows the GUI of the PPSD analysis tool, in which seismic noise has been analyzed on continuous data recorded on three channels from three different stations over a period of two months. The users can modify the display settings (Fig. 9a)

Figure 5. Seismic moment tensor module. (a) Parameterization widgets and additional action buttons to run the inversion and plotting seismograms and stations map and (b) widget to show the inversion results. CLVD, compensated linear vector dipole; DC, double-couple; ISO, isotropic. The color version of this figure is available only in the electronic edition.

to visualize the PPSDs or the diurnal and seasonal variation in the plotting widget (Fig. 9b).

Data retrieval. The data retrieval tool (Fig. S4) can be used to request data from FDSN or Earthworm servers, using ObsPy's client class. Data servers can be queried for continuous data or for earthquake recordings. In the latter case, the user can download an event catalog from an institution of their choice. For each selected event, *P*-wave arrival times at each station are estimated using the TauP library, and the waveforms are downloaded between a set amount of time before and after the estimated *P*-wave onset. The data retrieval GUI can also be used to download and save instrument responses for later use.

Synthetic seismograms. The synthetic seismogram tool allows the user to easily compute and download synthetic waveforms for a set of sources and receivers using Syngine, the Incorporated Research Institutions for Seismology Synthetics



Engine (see [Data and Resources](#)) and ObsPy, through a dedicated GUI. Syngine generates the Green's functions using AxiSem (Nissen-Meyer *et al.*, 2014), an axisymmetric spectral element method for 3D anelastic, anisotropic, and acoustic wave propagation in spherical domains, whereas the synthetic seismograms are calculated using Instaseis (van Driel *et al.*, 2015) for different Earth models. The available Earth models for these computations are explained in Syngine. The synthetic seismograms GUI can be used to visualize the synthetic waveforms

Figure 6. Main view of the receiver function analysis module. (a) H-k stacking and crustal thickness determination, (b) common conversion point (CCP) stack using the receiver functions shown in the H-k frame, and (c) cross section. The color version of this figure is available only in the electronic edition.

for different focal parameters, which can be plotted in a map. Figure 10a,b shows the visualization GUI and the synthetic generation dialog, respectively.

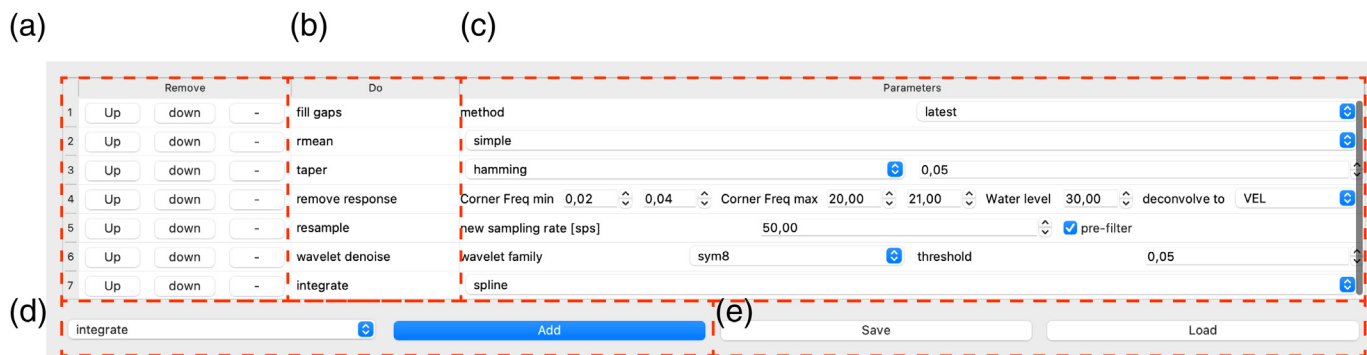


Figure 7. Macro frame. Example of a macro with seismic signal processing steps. (a) Widgets to set the order of the processing steps, (b) the processing type and (c) to set the parameters for each processing step. (d) Selection of processing steps to be

added into the macro and (e) widgets to save and load previously set macros. The color version of this figure is available only in the electronic edition.

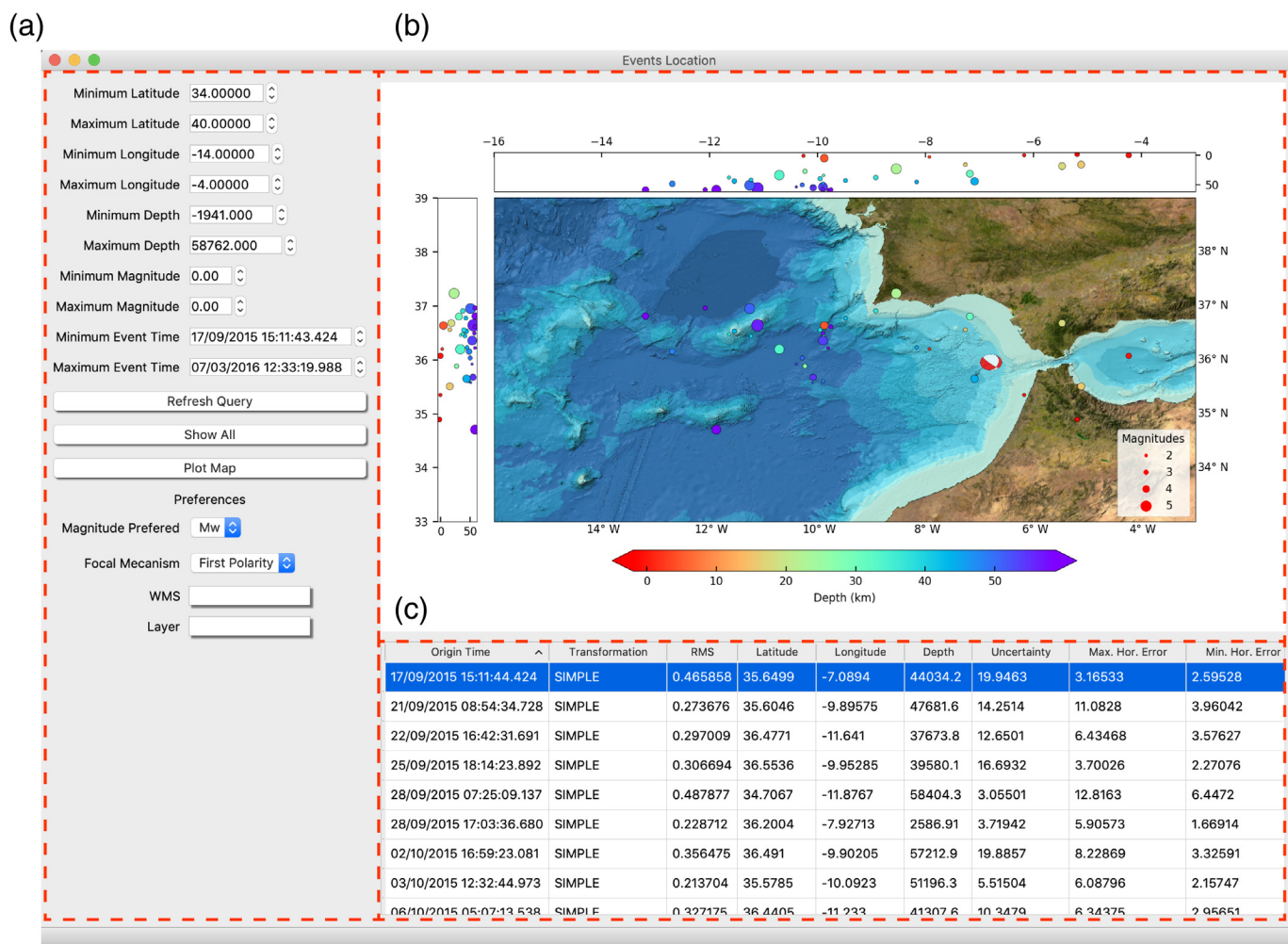
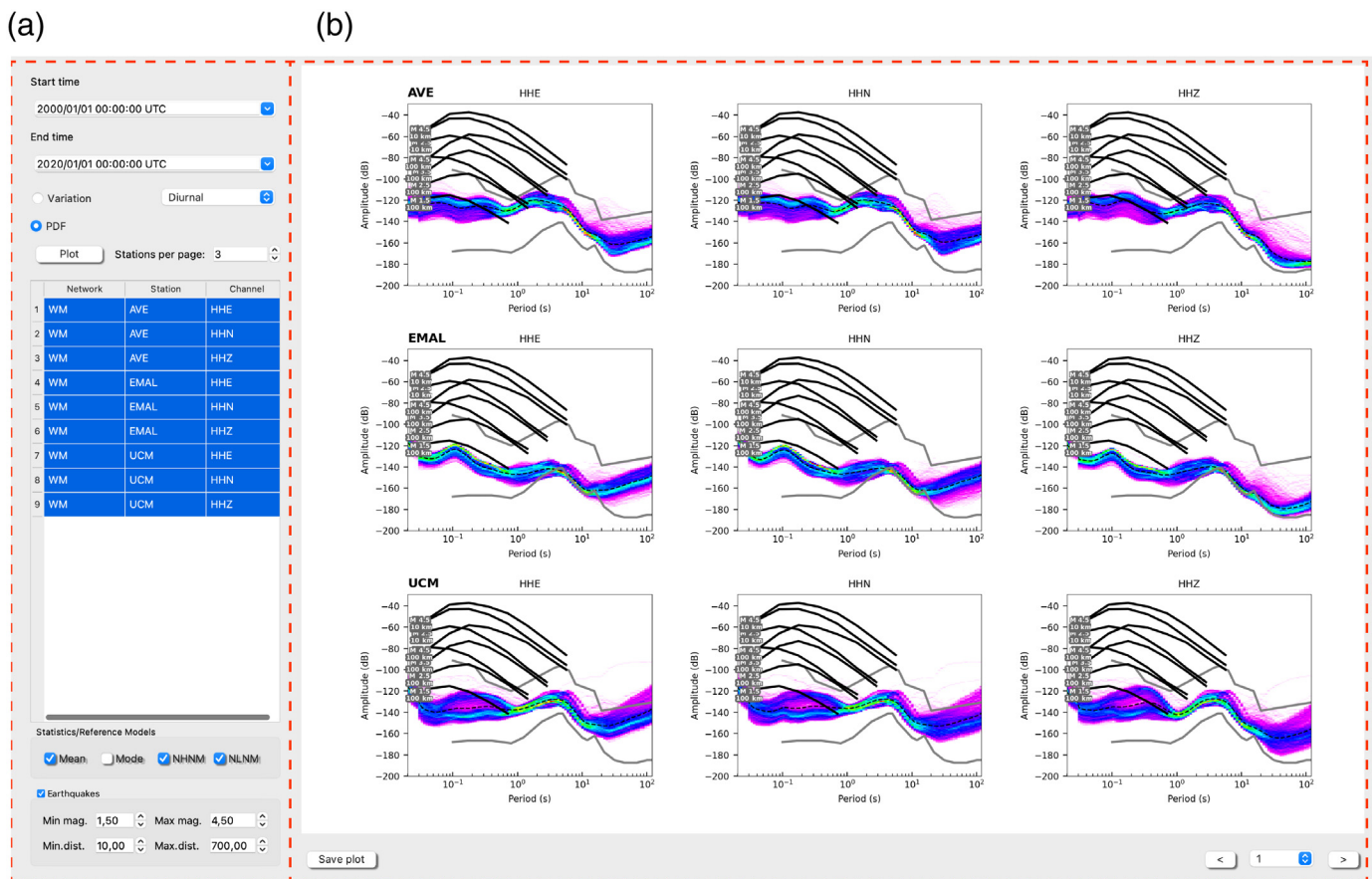


Figure 8. Database manager. (a) Widget to set a filter search, (b) map with the database plots, and (c) database table

attributes. The color version of this figure is available only in the electronic edition.



Future Development

The core and the functionality of ISP have been thoroughly tested. The ISP repository includes a wide variety of test examples gathered from publicly available seismic networks, including regional and teleseismic earthquakes, nuclear explosion recordings, and empirical Green's functions. As well as being useful for verifying that the software is working correctly, these data examples are used as a tutorial for new users.

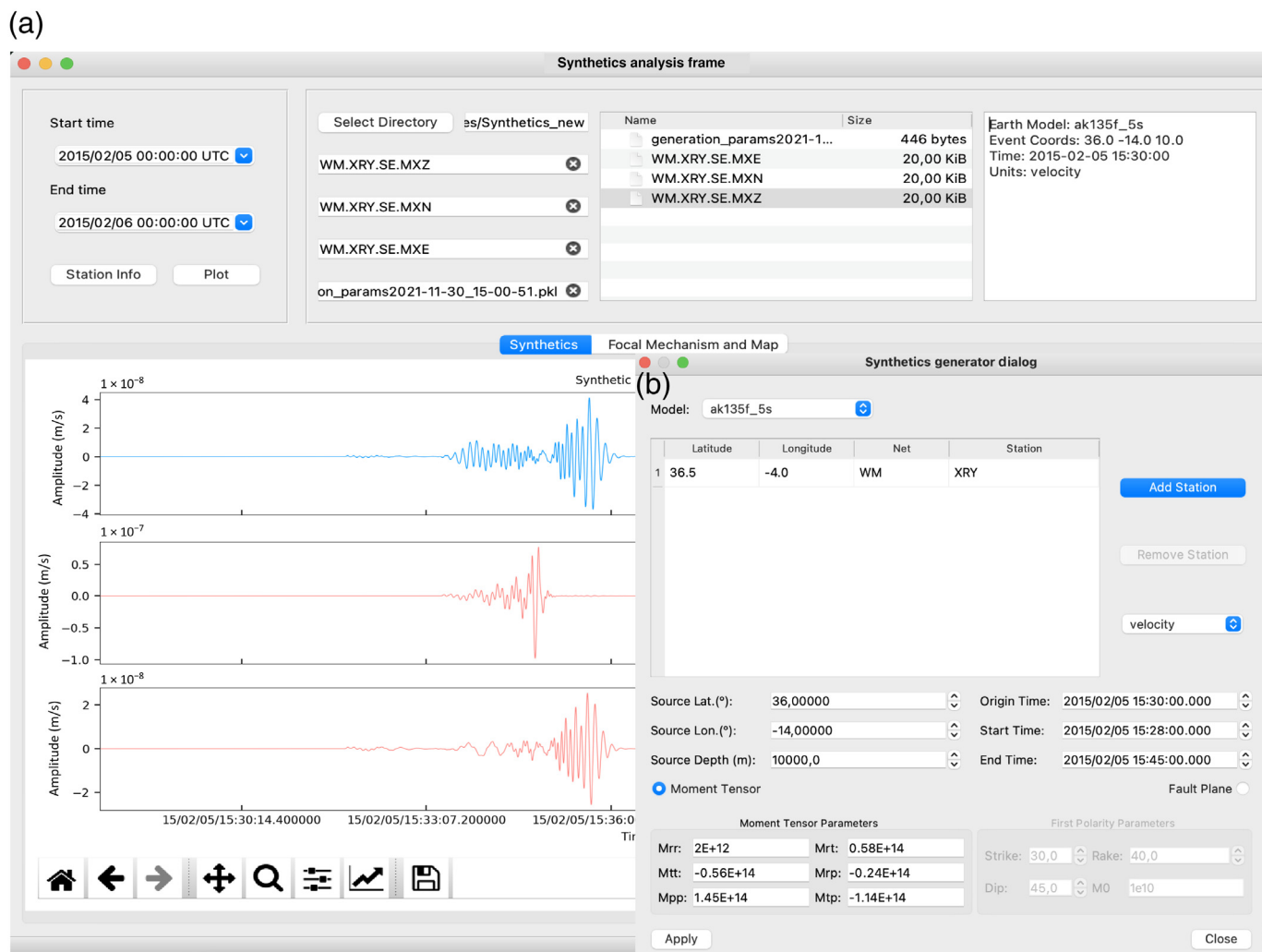
Because they are independent, all modules of ISP can be run at the same time, allowing the user to use the different processing routines simultaneously. Some highly demanding routines are performed in multiple threads to avoid interference between the events in each module. Some signal processing tools (such as prewhitening or spectrogram computation) are run in parallel jobs to boost the overall performance.

The modular approach of ISP simplifies the continued development of new tools and will thus allow for its functionality to grow and evolve over time. The current ISP design is focused on a thorough non-real-time earthquake analysis and offers a broad variety of algorithms and routines for this purpose. Nevertheless, a module aimed at the analysis of real-time data streams is being developed and will be implemented in the near future. Even though progress has been made to allow the near-real-time retrieval of data, it is still necessary to develop a specific tool to link the earthquake analysis tools

Figure 9. Probability power spectral density function (PPSD) framework. Shown is an example of a probability density function (PDF) visualization from a database with three components at each of three stations. (a) Widgets to set PPSD plotting parameters and (b) plotting widget to visualize PPSDs and diurnal or seasonal variations. The color version of this figure is available only in the electronic edition.

(e.g., automatic earthquake location, magnitude estimation, moment tensor inversion, slowness vector estimation, etc.) with the collected data.

In addition, we plan to expand ISP's capabilities toward imaging the Earth at different scales through the inclusion of a seismic ambient noise-related module. The study of ambient seismic noise and its properties is a computationally demanding task. There are only a few freely available packages written in Python to study ambient seismic noise (e.g., [Lecocq et al., 2014](#); [Goutorbe et al., 2015](#); [Jiang and Denolle, 2020](#)), and all of them are designed as command line tools. Nevertheless, implementing such a module should be specifically done either in a low-level language (i.e., C, Fortran, and Julia) or in Cython (i.e., C-extension for Python) so that the large amount of data often used in seismic noise tomography studies (>1 TB size) can be processed in a reasonable amount of time.



Conclusions

ISP is a modular, GUI-equipped compilation of software aimed at providing a user-friendly environment for performing diverse tasks in earthquake seismology. As of now, ISP includes modules aimed at earthquake location, focal parameter determination, computation and analysis of ARFs, representation and analysis of signals in the time–frequency domain, moment tensor inversion, and receiver function analysis. The graphical environment will allow a wide variety of researchers, from students with no coding experience to experienced data analysts, to use the provided algorithms and obtain useful results. The structure of ISP and its collaborative development environment will allow its functionality to be easily extended in the future by creating and/or incorporating new modules and tools.

Data and Resources

Integrated Seismic Program (ISP) is freely available at <https://github.com/ProjectISP/ISP> (last accessed February 2022). A complete tutorial for ISP can be found at https://projectisp.github.io/ISP_tutorial.github.io/ (last accessed February 2022), as well as real-data examples for each

Figure 10. (a) Synthetic seismogram analysis based on the (b) synthetic generator dialog. The color version of this figure is available only in the electronic edition.

of the modules. The tutorial also includes links to the Python libraries that support the software. ISP makes use of the ObsPy library (Krischer *et al.*, 2015) and the graphical user interfaces are built upon the PyQt5 library (<https://www.riverbankcomputing.com>, last accessed November 2021). The graphics are plotted using Matplotlib (Hunter, 2007), and the maps are generated using Cartopy (<https://scitools.org.uk/cartopy/>, last accessed November 2021). Multitaper coherence has been implemented using the Python library NiTime (<https://nipy.org/nitime/>, last accessed December 2021). Waveform data used to test ISP were retrieved from the Western Mediterranean network (<https://doi.org/10.14470/jz581150>), the Instituto Geográfico Nacional (IGN, <https://doi.org/10.7914/sn/es>, last accessed December 2021), the Instituto Português do Mar e da Atmosfera (IPMA, <https://doi.org/10.7914/sn/pm>), and Global Seismograph Network—Incorporated Research Institutions for Seismology and U.S. Geological Survey (IRIS and USGS; <https://doi.org/10.7914/SN/IU>). Other relevant data and resources were obtained from the following websites:

SeisGram2K (<http://alomax.free.fr/seisgram/SeisGram2K.html>, last accessed December 2021), FOCal MECHANism determinations (FOCMEC) (<https://seiscode.iris.washington.edu/projects/focmec>, last accessed December 2021), MkdDocs (<https://www.mkdocs.org/>, last accessed December 2021), SQLAlchemy (<https://www.sqlalchemy.org/>, last accessed December 2021), and Syngine (<http://ds.iris.edu/ds/products/syngine/>, last accessed November 2021). The supplemental material includes a short description of the following ISP tools: Polarization Analysis, Array Response Function, Vespagram, and Data Retrieval toolbox.

Declaration of Competing Interests

The authors acknowledge that there are no conflicts of interest recorded.

Acknowledgments

Funding was provided by the Spanish Navy Observatory, and this work was supported in part by the Spanish Ministerio de Economía, Industria y Competitividad project CGL2013-45724-C3-3 R and from the European Regional Development Fund (ERDF), Junta de Andalucía-Consejería de Economía y Conocimiento, Proyecto A-TIC-215-UGR18. Data from Landslide Assessment in the Spanish Navy Observatory (LASNO) project (Grant Number GIPP202017) in collaboration with the Geophysical Instrumentation Pool Potsdam (GIPP) of the GeoForschungsZentrum (GFZ, Potsdam) were used to test Integrated Seismic Program (ISP).

References

- Boashash, B., and P. Black (1987). An efficient real-time implementation of the Wigner-Ville distribution, *IEEE Trans. Acoust. Speech Signal Process.* **35**, no. 11, 1611–1618.
- Bormann, P., and J. W. Dewey (2012). The new IASPEI standards for determining magnitudes from digital data and their relation to classical magnitudes, in *New Manual of Seismological Observatory Practice 2 (NMSOP-2)*, Deutsches GeoForschungsZentrum GFZ, Potsdam, Germany, 1–44.
- Cabieces, R., E. Buforn, S. Cesca, and A. Pazos (2020). Focal parameters of earthquakes offshore Cape St. Vincent using an amphibious network, *Pure Appl. Geophys.* doi: [10.1007/s00024-020-02475-3](https://doi.org/10.1007/s00024-020-02475-3).
- Capon, J. (1969). High-resolution frequency-wavenumber spectrum analysis, *Proc. IEEE* **57**, no. 8, 1408–1418.
- Clinton, J. F., and T. H. Heaton (2002). Potential advantages of a strong-motion velocity meter over a strong-motion accelerometer, *Seismol. Res. Lett.* **73**, no. 3, 332–342.
- Daubechies, I. (1992). *Ten Lectures on Wavelets*, Society for industrial and applied mathematics, doi: [10.1137/1.9781611970104](https://doi.org/10.1137/1.9781611970104).
- Flinn, E. A. (1965). Signal analysis using rectilinearity and direction of particle motion, *Proc. IEEE* **53**, no. 12, 1874–1876.
- Font, Y., H. Kao, S. Lallemand, C.-S. Liu, and L.-Y. Chiao (2004). Hypocentre determination offshore of eastern Taiwan using the Maximum Intersection method, *Geophys. J. Int.* **158**, no. 2, 655–675.
- Gal, M., A. M. Reading, S. P. Ellingsen, K. D. Koper, S. J. Gibbons, and S. P. Nasholm (2014). Improved implementation of the fk and Capon methods for array analysis of seismic noise, *Geophys. J. Int.* **198**, no. 2, 1045–1054, doi: [10.1093/gji/ggu183](https://doi.org/10.1093/gji/ggu183).
- Goldstein, P., D. Dodge, M. Firpo, and L. Minner (2003). SAC2000: Signal processing and analysis tools for seismologists and engineers, in *The IASPEI International Handbook of Earthquake Engineering and Seismology*, W. H. K. Lee, H. Kanamori, P. C. Jennings, and C. Kisslinger (Editors), Vol. 81, Academic Press, London, United Kingdom, 1613–1620, doi: [10.1016/S0074-6142\(03\)80284-X](https://doi.org/10.1016/S0074-6142(03)80284-X).
- Goutorbe, B., D. L. de Oliveira Coelho, and S. Drouet (2015). Rayleigh wave group velocities at periods of 6–23 s across Brazil from ambient noise tomography, *Geophys. J. Int.* **203**, no. 2, 869–882.
- Havskov, J., P. H. Voss, and L. Ottemoller (2020). Seismological observatory software: 30 Yr of SEISAN, *Seismol. Res. Lett.* **91**, no. 3, 1846–1852, doi: [10.1785/0220190313](https://doi.org/10.1785/0220190313).
- Herrmann, R. B. (2013). Computer programs in seismology: An evolving tool for instruction and research, *Seismol. Res. Lett.* **84**, no. 6, 1081–1088, doi: [10.1785/0220110096](https://doi.org/10.1785/0220110096).
- Hunter, J. D. (2007). Matplotlib: A 2D graphics environment, *Comput. Sci. Eng.* **9**, no. 3, 90–95, doi: [10.1109/MCSE.2007.55](https://doi.org/10.1109/MCSE.2007.55).
- Jiang, C., and M. A. Denolle (2020). NoisePy: A new high-performance Python tool for ambient-noise seismology, *Seismol. Res. Lett.* **91**, no. 3, 1853–1866, doi: [10.1785/0220190364](https://doi.org/10.1785/0220190364).
- Krischer, L., T. Megies, R. Barsch, M. Beyreuther, T. Lecocq, C. Caudron, and J. Wassermann (2015). ObsPy: A bridge for seismology into the scientific Python ecosystem, *Comput. Sci. Discov.* doi: [10.1088/1749-4699/8/1/014003](https://doi.org/10.1088/1749-4699/8/1/014003).
- Langston, C. A. (1979). Structure under Mount Rainier, Washington, inferred from teleseismic body waves, *J. Geophys. Res.* **84**, no. B9, 4749–4762.
- Lecocq, T., C. Caudron, and F. Brenguier (2014). MSNoise, a Python package for monitoring seismic velocity changes using ambient seismic noise, *Seismol. Res. Lett.* **85**, no. 3, 715–726.
- Loeliger, J., and M. McCullough (2012). *Version Control with Git: Powerful Tools and Techniques for Collaborative Software Development*, O'Reilly Media, Inc, ASIN: 1449316387.
- Lomax, A., and A. Curtis (2001). Fast, probabilistic earthquake location in 3D models using oct-tree importance sampling, *Geophys. Res. Abstr.* **3**, 955.
- Mallat, S. (2009). *A Wavelet Tour of Signal Processing*, Third Ed., Academic Press, Inc., USA, ISBN: 9780123743701.
- McNamara, D. E., and R. P. Buland (2004). Ambient noise levels in the continental United States, *Bull. Seismol. Soc. Am.* doi: [10.1785/012003001](https://doi.org/10.1785/012003001).
- Nawab, S., F. Dowla, and R. Lacoss (1985). Direction determination of wideband signals, *IEEE Trans. Acoust. Speech Signal Process.* **33**, no. 5, 1114–1122.
- Nissen-Meyer, T., M. van Driel, S. C. Stähler, K. Hosseini, S. Hempel, L. Auer, A. Colombi, and A. Fournier (2014). AxiSEM: Broadband 3-D seismic wavefields in axisymmetric media, *Solid Earth* **5**, 425–445, doi: [10.5194/se-5-425-2014](https://doi.org/10.5194/se-5-425-2014).
- Peterson, J. R. (1993). Observations and modeling of seismic background noise, *U.S. Geol. Surv. Open-File Rept.* 93-322, doi: [10.3133/ofr93322](https://doi.org/10.3133/ofr93322).
- Podvin, P., and I. Lecomte (1991). Finite difference computation of traveltimes in very contrasted velocity models: A massively parallel approach and its associated tools, *Geophys. J. Int.* **105**, no. 1, 271–284.

- Prieto, G. A., R. L. Parker, and F. L. Vernon (2009). A Fortran 90 library for multitaper spectrum analysis, *Comput. Geosci.* doi: [10.1016/j.cageo.2008.06.007](https://doi.org/10.1016/j.cageo.2008.06.007).
- Ross, Z. E., M.-A. Meier, E. Hauksson, and T. H. Heaton (2018). Generalized seismic phase detection with deep learning, *Bull. Seismol. Soc. Am.* **108**, no. 5A, 2894–2901, doi: [10.1785/0120180080](https://doi.org/10.1785/0120180080).
- Rost, S., and C. Thomas (2002). Array seismology: Methods and applications, *Rev. Geophys.* **40**, no. 3, 2–27.
- Ruigrok, E., S. Gibbons, and K. Wapenaar (2017). Cross-correlation beamforming, *J. Seismol.* **21**, no. 3, 495–508.
- Sambridge, M. (2013). A parallel tempering algorithm for probabilistic sampling and multimodal optimization, *Geophys. J. Int.* **196**, no. 1, 357–374, doi: [10.1093/gji/ggt342](https://doi.org/10.1093/gji/ggt342).
- Sambridge, M., and K. Mosegaard (2002). Monte Carlo methods in geophysical inverse problems, *Rev. Geophys.* **40**, no. 3, 3–29.
- Schimmel, M., and H. Paulssen (1997). Noise reduction and detection of weak, coherent signals through phase-weighted stacks, *Geophys. J. Int.* doi: [10.1111/j.1365-246X.1997.tb05664.x](https://doi.org/10.1111/j.1365-246X.1997.tb05664.x).
- Smith, W. S., Z. Zeng, and J. Currence (2018). Seismology software: State of the practice, *J. Seismol.* **22**, no. 3, 755–788.
- Silva, S., P. Terrinha, L. Matias, J. C. Duarte, C. Roque, C. R. Ranero, W. H. Geisslerh, and N. Zitellini (2017). Micro-seismicity in the Gulf of Cadiz: Is there a link between micro-seismicity, high magnitude earthquakes and active faults? *Tectonophysics* doi: [10.1016/j.tecto.2017.07.026](https://doi.org/10.1016/j.tecto.2017.07.026).
- Stammler, K. (1993). SeismicHandler—Programmable multichannel data handler for interactive and automatic processing of seismological analyses, *Comput. Geosci.* **19**, no. 2, 135–140.
- Thomson, D. J. (1982). Spectrum estimation and harmonic analysis, *Proc. IEEE* **70**, no. 9, 1055–1096.
- Torrence, C., and G. P. Compo (1998). A practical guide to wavelet analysis, *Bull. Am. Meteorol. Soc.* doi: [10.1175/1520-0477\(1998\)079<0061:APGTWA>2.0.CO;2](https://doi.org/10.1175/1520-0477(1998)079<0061:APGTWA>2.0.CO;2).
- Vackář, J., J. Burjáněk, F. Gallovič, J. Zahradník, and J. Clinton (2017). Bayesian ISOLA: New tool for automated centroid moment tensor inversion, *Geophys. J. Int.* **210**, no. 2, 693–705, doi: [10.1093/gji/ggx158](https://doi.org/10.1093/gji/ggx158).
- van Driel, M., L. Krischer, S. C. Stähler, K. Hosseini, and T. Nissen-Meyer (2015). Instaseis: Instant global seismograms based on a broadband waveform database, *Solid Earth* **6**, no. 2, 701–717, doi: [10.5194/se-6-701-2015](https://doi.org/10.5194/se-6-701-2015).
- Ventosa, S., M. Schimmel, and E. Stutzmann (2017). Extracting surface waves, hum and normal modes: Time-scale phase-weighted stack and beyond, *Geophys. J. Int.* doi: [10.1093/gji/ggx284](https://doi.org/10.1093/gji/ggx284).
- Wathelet, M., J. L. Chatelain, C. Cornou, G. D. Giulio, B. Guillier, M. Ohrnberger, and A. Savvaidis (2020). Geopsy: A user-friendly open-source tool set for ambient vibration processing, *Seismol. Res. Lett.* **91**, no. 3, 1878–1889.
- Zhou, H. (1994). Rapid three-dimensional hypocentral determination using a master station method, *J. Geophys. Res.* **99**, no. B8, 15,439–15,455.
- Zhu, L., and H. Kanamori (2000). Moho depth variation in southern California from teleseismic receiver functions, *J. Geophys. Res.* **105**, no. B2, 2969–2980.

Appendix

The SQLite database included in Integrated Seismic Program (ISP), accessible through the Database tool, is designed to store the focal parameters (including the results of moment tensor inversions) and slowness vectors computed by the user. Figure A1 shows the structure of the database in detail.

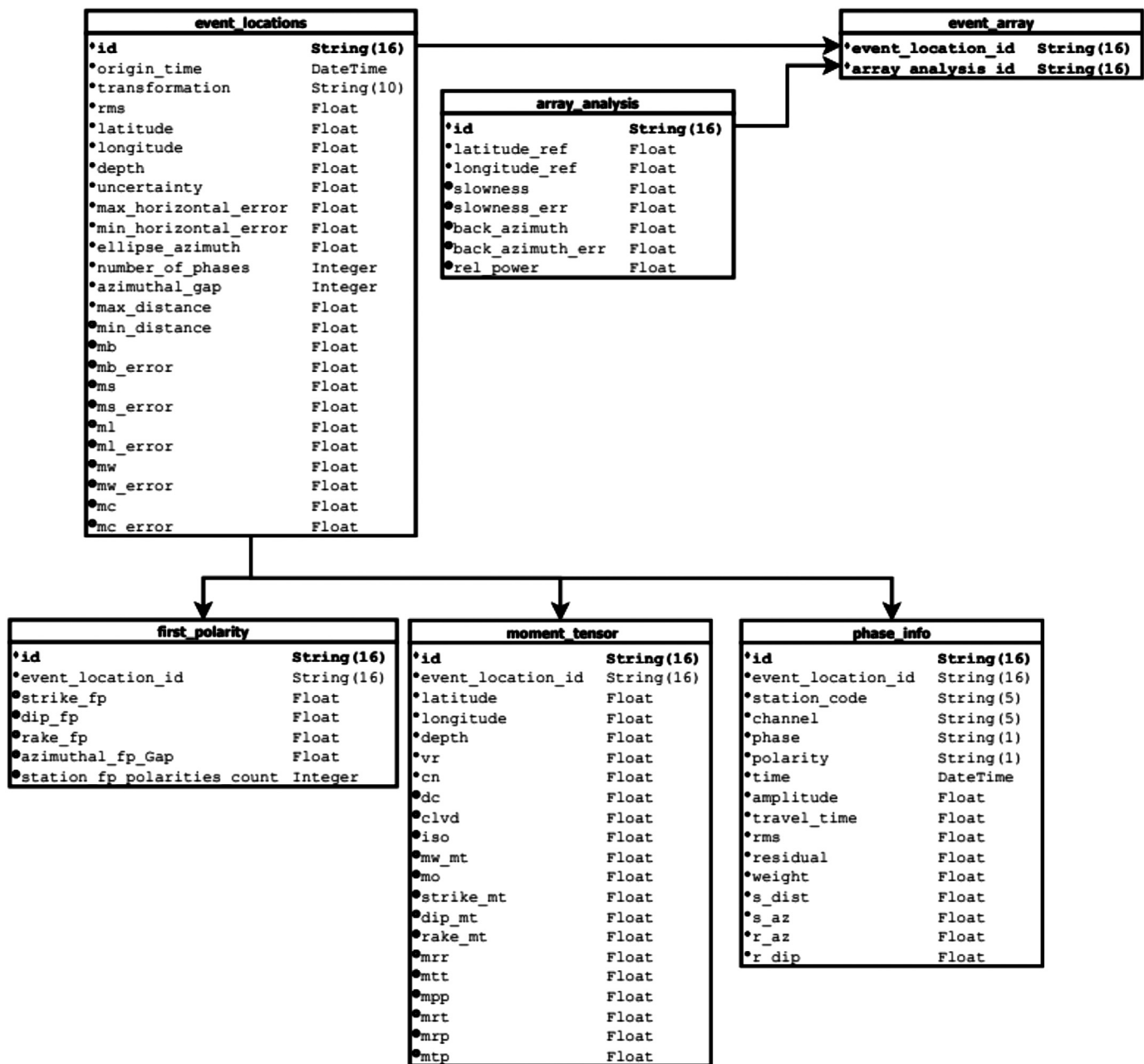


Figure A1. Structure of the Integrated Seismic Program (ISP) database and its connections to the main modules.

Manuscript received 29 July 2021
Published online 9 March 2022